ICAS 2020 SHANGHAI
International Council of the Aeronautical Sciences
32nd Congress of the International Council of the Aeronautical Sciences
September 6-10, 2021
Pudong Shangri-La, Shanghai, China

A STOCHASTIC ROBUSTNESS VERIFICATION OF NLG SIMPLE ADAPTIVE SHIMMY SUPPRESSION SYSTEM

A. Alaimo[1] & C. Orlando[1]

[1]Facoltà di Ingegneria e Architettura, Università di Enna Kore, Cittadella Universitaria, 94100, Enna, Italy

Abstract

The shimmy vibration is among the causes of reduction of the nose landing gear (NLG) fatigue life. Usually, the shimmy vibration problem is mitigated by installing passive dampers on the NLG , however, both semi-active and active shimmy suppression systems are currently investigated looking for better damping performance. The present work presents the design and numerical investigation of an active shimmy suppression system based on the simple adaptive control technique. Despite of the good results obtained during the design of the controller, it is to be taken into account that the controller designed for the nominal system may not be optimal for the actual working condition. For instance, environmental conditions influence the tire-road interaction while systems failures or wear can reduce the NLG stiffness and damping properties, moreover the taxiing speed and the system weight are varying parameters as well. The ultimate goal of the present work is the performance robustness analysis of the proposed simple adaptive shimmy suppression system under parameters uncertainties by means of Stochastic Robustness Analysis

Keywords: NLG Shimmy; Simple Adaptive Control; Stochastic Robustness Verification

1. Introduction

The self-sustained oscillations of the nose landing gear fork-wheel assembly around the steering axis are referred to as shimmy vibration . This phenomenon gets energy from the tire road interaction, thus it depends on the pavement and tire tread states as well as on the environmental conditions. Moreover, the shimmy behavior is also influenced by other mechanic parameters such as the stiffness and the damping capability of the strut but also the weight that acts on the system modifies the NLG shimmy behavior as it plays a direct role on the force and torque that are produced by the tire-road interaction. Last, a key role is played by the taxiing speed since there exist a critical advancing velocity above which the shimmy oscillations onset and the friction actions between the tire and road are no longer able to damp energy but, on the contrary, sustain the vibrations [1].

It is to be noted that the shimmy vibrations may be dangerous since they reduce the fatigue life of the NLG structural elements, cause wear of components with the consequence of free-play occurrence and, in the worst case, may stress the leg until its structural failure [2].

The shimmy problem is usually tackled by installing passive elements that allow to damp energy out of the vibrating system. Concepts of passive shimmy damper has been recently studied by [3].

However, considering the technological advancement toward the more or all electric aircraft [4], alternative solutions to the passive ones are under investigation. Generally speaking, the alternatives to the passive shimmy dampers are represented by the semi-active and by the active damping systems. The former has been sought for by studying magneto-rheological damping systems. An example can be found in [5]. The latter takes advantage of the steering system lead by electro-mechanical actuators and foresee for the implementation of active or adaptive control systems. Some examples of adaptive damping system are represented by [6, 7]

In the present work, an adaptive damping system based on the simple adaptive control SAC strategy is used [8, 9].

The SAC is a simplification of the Model Reference Adaptive MRAC scheme; in detail, the SAC controls the plant by using an adaptive output feedback signal and two adaptive feed-forward signals. A reference model, whose order can be different from the plant order, is used to generate the adaptive control signals: the feedback one employs the reference model output to define the tracking error to be zeroed while the feed-forward ones use the reference model state and input signals.
To safely apply the SAC scheme avoiding possible instabilities caused by the gain adaptation, it is requested that the plant to be controlled satisfies the so-called Almost Strict Passive ASP conditions. Unfortunately, most of the actual plant are not ASP. To solve such issue, a PArallel Feed-forward Compensator PFC can be added to plant in such a way that the augmented system becomes ASP. For more detail about the SAC, ASP conditions and PFC schemes, the interested reader is referred to literature [10].
The objective of the present work is to study the performance robustness of a shimmy suppression systems based on the SAC approach [8]. To do so, a probabilistic Monte Carlo approach is employed by means of the Stochastic Robustness Analysis SRA [11].
The SRA approach asks for the definition of performance indexes and criteria and then it foresee the computation of violating such criteria by using Monte Carlo analysis. By using the SRA, it is thus possible to analyse the performance robustness of the proposed simple adaptive shimmy suppression system taking into account parameters uncertainties that can be due, for instance, to environmental conditions or to wear of components.

2. Model description

For the sake of completeness, this section briefly recalls the equations that govern the NLG shimmy behavior under the assumptions taken into account. Successively, it reports the controller architecture along with the conditions to be met for its stable implementation. For more details about the model, the simple adaptive control approach and its stability proof, the interested reader is referred to literature [8, 9].
To carry out the stochastic robustness analysis of the shimmy simple adaptive suppression system, a three degree of freedom model of the nose landing gear rotational dynamics is considered.
A simplified drawn of the considered system is given in Figure 1.
More in detail, the kinematic variables used to describe the system dynamic are the NLG fork-wheel rotation angle ψ, its rate of change $\dot{\psi}$ and the tire side-slip angle α. These three variables are used to write the rotational equilibrium equation of the NLG assembly and the lateral dynamic equation of the tire, which is here modeled by means of the elastic string theory [1]. The rotational equilibrium equation and the tire elastic string model are then written in space state form by introducing the state vector $\mathbf{x} = \{\psi, \dot{\psi}, \alpha\}^T$; it is written as

$$\begin{aligned}
\begin{bmatrix} \dot{\psi} \\ \ddot{\psi} \\ \dot{\alpha} \end{bmatrix} &= \begin{bmatrix} 0 & 1 & 0 \\ -\frac{K_E}{J} & -\frac{1}{J}\left(K_D - \frac{\kappa}{V}\right) & \frac{W}{J}\left(c_M - e c_F\right) \\ \frac{V}{3a} & \frac{e-a}{3a} & -\frac{V}{3a} \end{bmatrix} \begin{bmatrix} \psi \\ \dot{\psi} \\ \alpha \end{bmatrix} + \begin{bmatrix} 0 & 0 & 0 \\ \frac{1}{J} & \frac{1}{J} & \frac{1}{J} \\ 0 & 0 & 0 \end{bmatrix} \begin{bmatrix} u \\ d \\ d_{NL} \end{bmatrix} \\
y &= \begin{bmatrix} 1 & 0 & 0 \end{bmatrix} \begin{bmatrix} \psi \\ \dot{\psi} \\ \alpha \end{bmatrix}
\end{aligned} \tag{1}$$

where K_E is the torsional leg stiffness provided by the scissor link, K_D is the inherent strut damping constant, J the mass moment of inertia of the whole system, e is the caster length, W is the weight that acts on the NLG and V is the taxiing speed. Moreover, $2a$ is the contact length between the tire and the pavement, κ is the constant of tread width tire moment while c_F and c_M are stiffiness related to the lateral force and self-aligning moment engendered by the tire-ground interaction. More insights about such parameters can be found in [12, 13]. In Eq. 1, $u(t)$ is the control moment applied by an electromechanical actuator, $d(t)$ is an externally applied disturbance torque while $d_{NL}(\mathbf{x},t) = M_Z(\alpha,\alpha_M) - eF_Y(\alpha,\alpha_F) - W(c_M - ec_F)\alpha$, being M_Z and F_Y the nonlinear self-aligning moment and lateral force introduced by tire-ground interaction and defined in terms of sideslip (α) and limiting (α_F and α_M) angles according to [8].
It is worth noting that, with the aim of tuning the simple adaptive controller, the system must have the same number of input and output, in contrast with Eq. 1. However, the knowledge of the disturbance

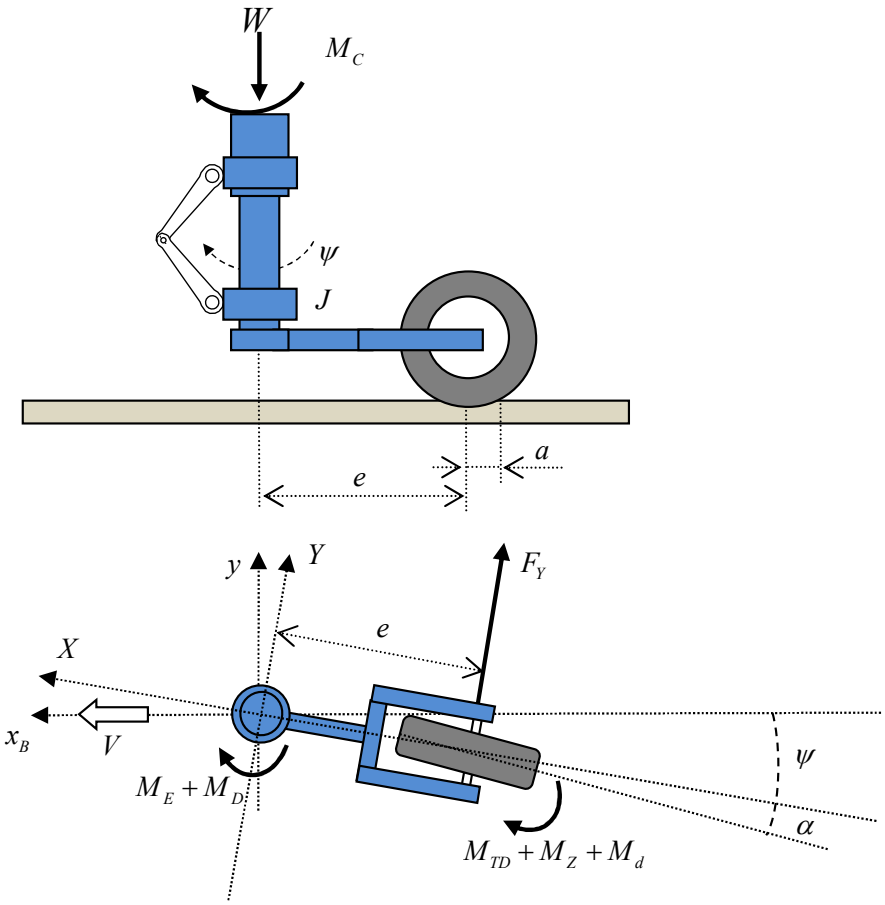

Figure 1 – Scheme of the NLG system.

is not requested during the controller design steps. This is true if the disturbance is bounded, as it is the present case. Thus, taking this last consideration into account, the plant governing equations can be written as a SISO transfer function that relates the fork-wheel rotation angle output to the control moment $u(t) = M_c(t)$ input. It follows that the SAC can be applied to the linearized plant and the nonlinear effects will be successively included as disturbance actions [14, 10].
The application of the SAC, alike the Model Reference Adaptive Control-MRAC, asks for the implementation of a reference model to be followed. Let's say that such stable reference model is

$$\begin{aligned} \dot{\mathbf{x}}_m(t) &= \mathbf{A}_m \mathbf{x}_m(t) + \mathbf{b}_m u_m(t) \\ y_m(t) &= \mathbf{c}_m^T \mathbf{x}_m(t) \end{aligned} \tag{2}$$

Differently from the MRAC, however, by employing SAC algorithm the plant is requested to follow the model reference output time history $y_m(t)$ instead of the evolution of its state $\mathbf{x}_m(t)$. This simplifies a lot the implementation of the SAC from both the software and hardware points of view: there is no need for state observer nor for online parameters identification, and the number of sensor devices to be installed into the actual plant is greatly reduced. For the proposed shimmy suppression system, such considerations imply the use of just one sensor of angular position to read the fork-wheel assembly rotation, thus reducing the number of sensors installation to one instead of three, with respect to a state feedback algorithm.
Moreover, it also follows that the number of state variables of the plant and that of the reference model can be different. Thus, the reference model is simply used as a signal generator that allows to define the output tracking error $e(t) = y_m(t) - y(t)$ to be zeroed by the controller that, in present case, leads the electromechanical actuator.
With this aim, the adaptive control signal is created as

$$u(t) = (K_{Pe} + K_{Ie})e(t) + (K_{Px} + K_{Ix})x_m(t) + (K_{Pu} + K_{Iu})u_m(t) \tag{3}$$

where K_P and K_I are the so-called proportional and integral adaptive gains that are defined, respectively, as

$$K_{Pe}(t) = \Gamma_{Pe} e(t)^2; \quad K_{Px}(t) = \Gamma_{Px} e(t) x_m(t); \quad K_{Pu}(t) = \Gamma_{Pu} e(t) u_m(t); \tag{4}$$

and

$$\dot{K}_{Ie}(t) + \sigma K_{Ie}(t) = \Gamma_{Ie} e(t)^2; \quad \dot{K}_{Ix}(t) = \Gamma_{Ix} e(t) x_m(t); \quad \dot{K}_{Iu}(t) = \Gamma_{Iu} e(t) u_m(t); \tag{5}$$

In Eqs. 4-5, the terms Γ are invariant gains to be properly tuned while the positive valued term σ is introduced to avoid the increase of the adaptive gain when the tracking error is zero. The crucial term for the stability of the controlled system is $K_{Ie}e(t)$ while the others are used to obtain the desired performance of the adaptive controlled system.

It is now to be said that, in order to have a stable SAC controlled system, the plant should be Almost Strict Passive ASP [10]. In the case of a SISO system, the ASP condition implies the Almost Strict Positive Realness ASPR of its transfer function $G(s)$. More in detail, a transfer function $G(s)$ is ASPR when the numerator polynomial is Hurwitz and its leading coefficient is positive, and the relative degree of $G(s)$ is 1. If the plant is not ASP, then the SAC controller should be applied to the plant properly augmented by means of a Parallel Feedforward Compensator PFC. Namely, for a SISO system the SAC must be applied to the augmented transfer function $G_a(s) = G(s) + G_{PFC}(s)$. The PFC should have low gain, such that the output of the augmented plant remains close to the output of the actual system [10].

A block diagram representation of the augmented NLG plant controlled by SAC according to reference model is shown in Figure 2.

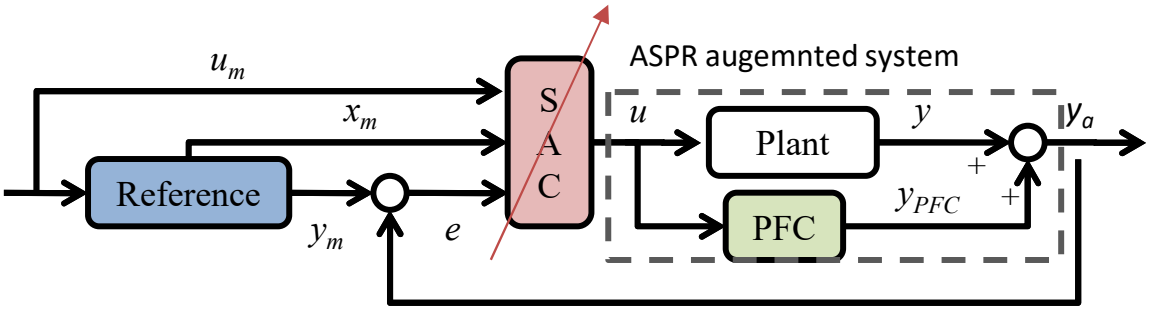

Figure 2 – Block diagram representation of the controlled system.

3. Study Case and Design Results

The study case considered in the present work is referred to into the literature as *Tire Damage*. A torque disturbance of $1\,kNm$ applies to the tire of the NLG at $t = 0.2\,s$ and lasts for $0.1\,s$. This study case has been previously used for the tuning of the PFC and of the invariant gains of the SAC in [8]. For the sake of completeness the design parameters are here reported. The plant linearized at the trimmed condition reported in Table 1 under the column $DM-$deterministic model has been considered.

In particular, the Tire Road Condition parameter is introduced to model, in a simplified way, the influence of wet and icy pavement. According to literature [15, 16], wet and icy conditions reduces the interaction of tire with the road with respect to the dry case. This phenomenon is modeled by simply multipling the cornering and the self-aligning stiffness, and limiting angles as well, by the parameter TRC which is assumed to vary in the interval $[0, 1]$: being the dry case represented by 1, the icy one represented by 0 while the intermediate values refer to different wet conditions. Values of TRC greater than unity could be used to model possible conditions characterized by a grip greater than usual.

The plant transfer function in such configuration is

$$G(s) = \frac{s + 266.67}{s^3 + 280.04s^2 + 1.0357 \times 10^5 s + 3.6267 \times 10^7} \tag{6}$$

Table 1 – Deterministic model data

Parameter	DM
Inertia of NLG - J $[kgm^2]$	1
Caster Length - e $[m]$	0.1
Forward velocity - V $[m/s]$	80
Weight - W $[kN]$	9
Torsional Stifness - K_E $[kNm/rad]$	100
Damping constant - K_D $[Nsm/rad]$	10
Half contact length - a $[m]$	0.1
Constant of tread width tire moment - κ $[Nm^2/rad]$	-270
Cornering stiffness - c_F $[rad^{-1}]$	20
Self-aligning stiffness - c_M $[rad^{-1}]$	-2
Limiting angle of Cornering Force - α_F $[deg]$	5
Limiting angle of Self-aligning Moment - α_M $[deg]$	10
Tire Road Condition - TRC	1

As it appears from Eq. 6, the numerator is Hurwitz and its leading coefficient is positive, however the relative degree of the transfer function is not 1. This implies that G(s) is not ASPR and, thus, in order to apply the simple adaptive control, the plant should be augmented by adding a parallel feedforward compensator. In accordance with [10], the PFC has been designed as the inverse of an high gain controller $C(S)$ that stabilize the plant transfer function $G(s)$. More in detail, the controller has been chosen as an ideal proportional-derivative one $C(s) = 160(1+10s)$. Then, by adding the inverse of $C(s)$ in parallel to the plant, the following ASPR transfer function of the plant in the trimmed configuration is obtained

$$G_a(s) = \frac{0.00625s^3 + 11.75s^2 + 3315s + 2.269 \times 10^5}{10s^4 + 2801s^3 + 1.036 \times 10^6 s^2 + 3.628 \times 10^8 s + 3.627 \times 10^7}. \tag{7}$$

Successively, with the aim of tuning the SAC invariant gains the following considerations have been done: the SAC is applied to simply damp the shimmy vibrations by maintaining the fork-wheel rotation angle to zero degree, thus the reference model output, state and input should be zero at any time instant. It follows that Γ_x and Γ_u are set to zero while $\Gamma_{Pe} = 10^7 Nm/deg^3$, $\Gamma_{Ie} = 10^8 Nm/deg^3 s$ and $\sigma = 0.001 s^{-1}$. The values of the invariant gains given before have been selected as the ones that minimize three time domain based performance indexes, namely the settling time T_s, the percentage overshoot PO and the maximum control moment M_{cMax} requested by the controller. For more insight about the controller and the PFC tuning approach and results, the interested reader is referred to [8]. Figure 3 shows the transient response of the NLG fork-wheel rotation angle considering the nonlinear model Eq. 1 with the disturbance moment of the $tire damage$ study case and the SAC and PFC tuned by using the aforementioned parameter.

The comparison with literature data show the soundness of the proposed approach, see Figure 3. The response of the minimal control synthesis scheme show an underdamped response while the SAC based controller manifests no oscillation. On the other hand, the zero average dynamics controller shows a bias rotation angle which is lower the one obtained by the proposed approach. It is worth noting however that proposed controller is based on an output feedback scheme in contrast with both the minimum control synthesis and the zero average dynamics schemes that ask for full-state feedback, thus requesting the implementation of more sensing devices and/or the design of state observers.

It appears from Figure 3 that: the percentage overshoot is $PO = 0$; the maximum rotation angle reached by the fork-wheel assembly is $\psi_{max} = 0.41 deg$ (which is far below the limit shimmy value of $1.5 deg$ given in [7]); the settling time is $T_s = 0.055$ considering $|\psi(t)| < 5 \times 10^{-3} deg$. Moreover, the maximum control moment requested by the SAC is $M_{cMax} = 1426 Nm$ which is lower than the actuator saturation of $2000 Nm$ [7].

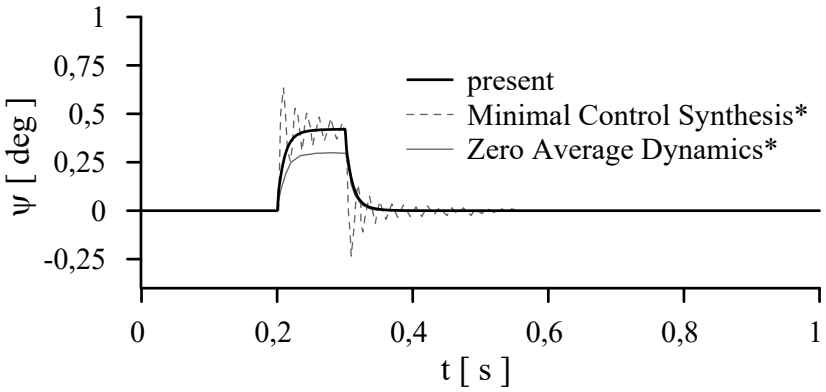

Figure 3 – Shimmy rotation time history comparison (* refer to [6]).

4. Performance Stochastic Robustness Analysis

Results obtained by using the deterministic model are valid and give an insight about the system behavior. However, system's parameters can vary because of several reasons even during operational life. Common reasons of uncertainty of parameters are related to environmental conditions and wear of components, among others. For instance, wear of torque link joining elements can cause a reduction of the torsion stiffness of the leg, whereas unusual wear of tire tread, as well as the variation of inflating pressure, can influence the NLG interaction with the ground. Moreover, environmental conditions can also affect the tire-ground contact dynamics leading to shimmying behavior possibly unforeseen by the deterministic model. The weight that acts on the NLG also plays a role since it can be different from the design case because of different operating conditions of the aircraft. The taxiing speed can change, as well, influencing shimmy response. The control system should however be able to adapt and damp the shimmy oscillation despite the parameters variation. To verify the simple adaptive shimmy suppression system robustness to parameters uncertainties, the Monte Carlo approach proposed in [11] is here employed.

More in detail, with the exception of the NLG inertia and of the caster length, all other parameters are considered as uncertain. Two different probabilistic model, referred to as $PM1$ and $PM2$, are built. The deterministic model parameters are the mean value of the probabilistic ones, exception made for the taxiing speed, whose mean value is set to $50\,m/s$, and the tire road condition index TRC who is let vary between 0 (icy road) and 1.2 (more grip than normal). To take into account the largest uncertainty, the maximum entropy principle is used and the uniform distribution is chosen as probability density function [17, 18]. It is clear that this assumption can results in an overly conservative verification of the controlled system behavior, different probability density distribution obtained by experimental campaign would of course be used if available. Table 2 reports the probabilistic model data in terms of minimum and maximum values.

To apply the SRA approach for verifying the simple adaptive shimmy suppression system, model parameters are selected randomly in the uncertainty domains and Monte Carlo evaluations are performed to solve the nonlinear equation of motions of the augmented plant controlled by the SAC scheme. The system transient response, computed during the MC simulations in term of fork-wheel rotation angle, is compared with a time domain envelope constraint that is built in accordance with the worst cases presented in [7]. It is worth noting that such worst case limits are far below the design requirements [7, 8]. The upper envelope constraint $U_e(t)$, in degree, is defined as

$$U_e(t) = \begin{cases} 1.0 & \text{if } t < 0.3s \\ -8t + 3.4 & \text{if } 0.3 \leq t \leq 0.4 \\ 0.2 & \text{if } t > 0.4 \end{cases} \tag{8}$$

Table 2 – Probabilistic model data

Parameter	$PM1\,[min, max]$	$PM2\,[min, max]$
Inertia of NLG - J $[kg\,m^2]$	1	1
Caster Length - e $[m]$	0.1	0.1
Forward velocity - V $[m/s]$	$[20, 80]$	$[5, 95]$
Weight - W $[kN]$	$[6.3, 11.7]$	$[4.95, 13.05]$
Torsional Stiffness - K_E $[kNm/rad]$	$[75, 125]$	$[62.5, 137.5]$
Damping constant - K_D $[Nsm/rad]$	$[7.5, 12.5]$	$[6.25, 13.75]$
Half contact length - a $[m]$	$[0.08, 0.12]$	$[0.07, 0.13]$
Constant of tread width tire moment - κ $[N\,m^2/rad]$	$[-216, -324]$	$[-189, -351]$
Cornering stiffness - c_F $[rad^{-1}]$	$[16, 24]$	$[14, 26]$
Self-aligning stiffness - c_M $[rad^{-1}]$	$[-1.6, -2.4]$	$[-1.4, -2.6]$
Limiting angle of Cornering Force - α_F $[deg]$	$[4, 6]$	$[3.5, 6.5]$
Limiting angle of Self-aligning Moment - α_M $[deg]$	$[8, 12]$	$[7, 13]$
Tire Road Condition - TRC	$[0, 1.2]$	$[0, 1.2]$

while the lower envelope limit is

$$L_e(t) = \begin{cases} -0.2 & \text{if } t < 0.3s \\ 3t - 1.4 & \text{if } 0.3 \leq t \leq 0.4 \\ -0.2 & \text{if } t > 0.4 \end{cases} \tag{9}$$

The likelihood of violating such envelope constraint $\hat{P}$, computed using all the MC evaluation, is used as a binomial metric of system performance robustness. Results in terms of likelihood of envelope violation are plotted in Figure 4 along with confidence interval for increasing number of Monte Carlo evaluations. With reference to $PM1$, it appears that the probability of violating the envelope constraint is $\hat{P} = 0$ with confidence interval$(0, 0.07)$ considering 5000 evaluations; this indicates the robustness of the controller under the $PM1$ case. On the other hand, values different than zero are shown by the $PM2$ results in Figure 4. After 3000 evaluation, the mean value of the likelihood of violating the constraint is almost constant and this means that the considered 5000 Monte Carlo simulations are enough to provide accurate statistical results. More in detail, the probability of violating the constraint is $\hat{P} = 0.0098$ with a confidence interval $(0.0089, 0.015)$.

Table 3 collects MC results obtained under the parameters' variation assumed in both the probabilistic models considered. In particular, looking at results of $PM2$, it can be seen that the control moment is always below the actuator saturation limit of $2\,kNm$ and the shimmy angle never reaches the upper limit envelope of $1\,deg$; on the other hand, the PO increases considerably with respect to $PM1$ results and, moreover, the maximum value of the settling time is almost three times larger than the one obtained under the $PM1$ model. This can suggest the presence of an oscillation which lasts longer and violates the envelope constraints.

To help visualizing this result, the envelopes of the 5000 MC transient responses are plotted in Figure 5 along with the segmented envelope constraint for both probabilistic models.

It is easy to note that the envelope constraint are never violated when the parameters' uncertainty are described by model $PM1$. On the contrary, the very wide uncertainty ranges considered by $PM2$ affect negatively the system response (with a probability of 0.98% of violating the constraints). In such case, the constraint is violated because the settling time is larger than expected.

To have an insight about what parameters have greatest influence on the NLG shimmy behavior dampened by SAC, the Spearman's ρ correlation matrix is given in Table 4.

According to literature [19, 20], the correlation can be considered low if the value of $\rho \geq 0.1$ and medium when $\rho \geq 0.3$, while the effect is large when $\rho \geq 0.5$. Looking at Table 4, it can be noted that the taxing speed has a medium effect on the PO, as the velocity increases the PO tends to decrease; the advancing speed also influences the maximum value of the control torque. The weight has small effect on the maximum rotation angle, PO and settling time.

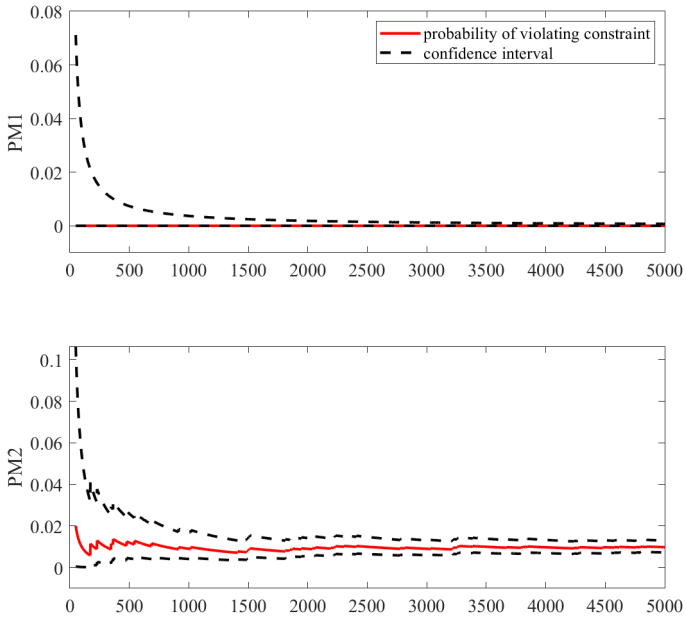

Figure 4 – Convergence of the Monte Carlo Stochastic Robustness Verification.

Table 3 – Probabilistic models summarizing results

PM1				
	$\psi_{max}\,[deg]$	PO	$T_s\,[s]$	$M_c max\,[Nm]$
min	0.401	-5.064	0.047	1346
max	0.611	-1.070	0.086	1392
mean	0.495	-2.790	0.066	1372
std	0.065	1.269	0.012	13
PM2				
	$\psi_{max}\,[deg]$	PO	$T_s\,[s]$	$M_c max\,[Nm]$
min	0.287	-10.701	0.018	1293
max	0.864	14.703	0.215	1536
mean	0.493	-1.972	0.068	1369
std	0.106	2.693	0.025	21

The stiffness has large effect on all of the investigated performance indexes: an increase of K_E implies a reduction of the rotation angle, of the settling time and of the control torque while its effect is positive on the percentage overshoot. This strong effect of the leg torsion stiffness is expected and it is in accordance with the literature.
On the contrary, the damping constant of the leg appears to have no effect; it is however to be put in highlight that the obtained correlation coefficients have no significance. Similar considerations can be drawn for the tire half-contact length a and the tread-width constant κ.
Last, looking at the parameters that describe the tire lateral force and the self-aligning moment, it can be concluded that they have medium effect on the system performance. As expected, similar effect is found for the parameter that represent the tire road interaction condition.
Eventually, the results obtained in terms of performance indexes during all the Monte Carlo evaluation are represented in Figure 6 as scatter plot to visualize their trend with respect to the uncertain parameters. The medium to large effects of some parameters' uncertainty on the performance metrics are clearly visible. Moreover, Figure 6 shows in red the cases for which the constraints are violated. Interestingly, it can be noted that they are almost randomly disperse for all the parameters with the exception of the taxiing speed. It is evident that all the cases of constraint violation are obtained when the NLG is supposed to travel at lowest value of speed. This is in accordance with results previously

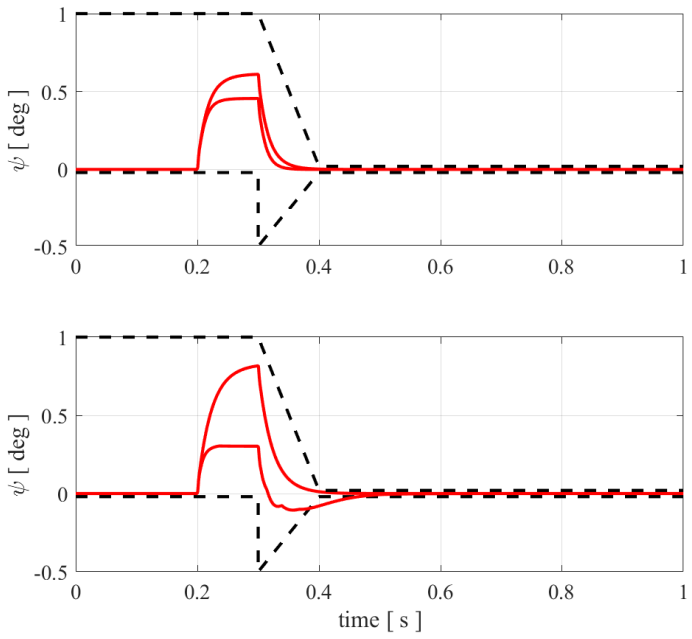

Figure 5 – Visualization of time histories envelops of the wheel angle.

find in [8]. Another interesting observation is drawn looking at the column of the settling time: all the violation cases shows values greater than 0.13.

Table 4 – Spearman's correlation matrix

	$\psi_{max}\,[deg]$	PO	$T_s\,[s]$	$M_c max\,[Nm]$
V	-0.062	-0.378	-0.113	0.299
W	-0.204	0.262	-0.181	-0.008*
K_E	-0.861	0.531	-0.614	-0.902
K_D	-0.015*	0.004*	-0.004*	-0.136
a	-0.016*	0.154	-0.020*	0.013*
κ	0.090	-0.074*	0.032*	0.144
c_F	-0.352	0.453	-0.331	0.027*
c_M	0.360	-0.443	0.333	-0.031*
α_F	-0.327	0.429	-0.315	0.031*
α_M	-0.336	0.434	-0.301	0.018*
TRC	-0.343	0.446	-0.323	0.035*

Note: * p > 0.05

5. Conclusions

A stochastic robustness analysis of an alternative shimmy suppression system for aircraft nose landing gear has been carried out in the present work. The shimmy damping system can take advantage of steering electro-mechanical actuators lead by a simple adaptive controller. The design of the SAC scheme and the tuning of the parallel feedforward compensator, needed to meet the almost strict passive condition, have been described. Two probabilistic model based on the maximum entropy principle have been built to consider different parameters uncertainty degrees. Monte Carlo SRA results have shown the performance robustness of the proposed simple adaptive shimmy suppression system showing a reduction of performance only at very low values of advancing speed.

6. Contact Author Email Address

caloger.orlando@unikore.it

7. Copyright Statement

References

[1] Somieski G. Shimmy analysis of a simple aircraft nose landing gear model using different mathematical methods. *Aerospace Science and Technology*, Vol. 1, No. 8, pp 545-555, 1997.

[2] Coetzee E. *Shimmy in aircraft landing gear*. Technical report, Problem presented by Airbus, 2006.

[3] Rahmani M, and Behdinan K. On the effectiveness of shimmy dampers in stabilizing nose landing gears. *Aerospace Science and Technology*, Vol. 91, pp 272-286, 2019.

[4] MARÉ JC, and FU J. Review on signal-by-wire and power-by-wire actuation for more electric aircraft. *Chinese Journal of Aeronautics*, Vol. 30, No. 3, pp 857-870, 2017.

[5] Chongxuan, K., Bo, W., and Shixing, Z. Design and Experiment of Magnetorheological Shimmy Damper Controller Based on Deep Neural Network. *CSAA/IET International Conference on Aircraft Utility Systems (AUS 2018)*, Guiyang, China, IET, pp 432–437, 2018.

[6] Burbano-L DA, Coraggio M, di Bemardo M, Garofalo F, and Pugliese M. Adaptive and quasi-sliding control of shimmy in landing gears. *2018 European Control Conference (ECC)*, Limassol, Cyprus,18274763, pp 563-568, 2018.

[7] Pouly G, Huynh TH, Lauffenburger JP, and Basset M. Feedback Fuzzy Adaptive Control for Active Shimmy Damping. *European Journal of Control*, Vol. 17, No. 4, pp 370–393, 2011.

[8] Orlando C. Nose landing gear simple adaptive shimmy suppression system. *Journal of Guidance, Control, and Dynamics*, Vol. 43, No. 7, pp 1298-1312, 2020.

[9] Alaimo A and Orlando C. Analysis of a shimming aircraft NLG controlled by the modified simple adaptive control. *Advances in aircraft and spacecraft science*, Vol. 7, No. 5, pp 459-473, 2020.

[10] Barkana I. Simple adaptive control–a stable direct model reference adaptive control methodology–brief survey. *International Journal of Adaptive Control and Signal Processing*, Vol. 28, No. 7-8, pp 567-603, 2014.

[11] Ray LR, Stengel RF. A monte carlo approach to the analysis of control system robustness. *Automatica*, Vol. 29, No. 1, pp 229–236, 1993.

[12] Pacejka H. *Tire and Vehicle Dynamics*. Elsevier, 2005.

[13] Besselink IJM. *Shimmy of Aircraft Main Landing Gears*. TUDelft, 2000.

[14] Omori Y, Suzuki S and Masui K. Flight Test of Fault-Tolerant Flight Control System Using Simple Adaptive Control with PID Compensator. *AIAA Infotech@Aerospace Conference*, Boston, Massachusetts, USA, AIAA Paper 2013-5210, 2013.

[15] Brewer H. Parameters Affecting Aircraft Tire Control Forces. *6th Aircraft Design, Flight Test and Operations Meeting*, Los Angeles,CA,U.S.A, AIAA Paper 1974-966, 1974.

[16] Sienel W. Estimation of the Tire Cornering Stiffness and its Application to Active Car Steering. *Proceedings of the 36th IEEE Conference on Decision and Control*, Piscataway, NJ,U.S.A, 5, pp 4744–4749, 1974.

[17] Shannon CE, Weaver W. *The Mathematical Theory of Communication*. University of Illinois Press, 2015.

[18] Cover TM, Thomas JA . *Elements of Information Theory*. John Wiley & Sons, 2012.

[19] Cohen J. *Statistical Power Analysis for the Behavioral Sciences*. Lawrence Erlbaum Associates, 1988.

[20] Alaimo A, Esposito A, Orlando C, and Simoncini A. Aircraft Pilots Workload Analysis: Heart Rate Variability Objective Measures and NASA-Task Load Index Subjective Evaluation. *Aerospace*, Vol. 7, No. 9, pp 137, 2020.

[21] Smith J, Jones B and Brown J. *The title of the book*. 1st edition, Publisher, 2001.

[22] Smith J, Jones B and Brown J. The title of the conference paper. *Proc Conference title*, where it took place, Vol. 1, paper number, pp 1-11, 2001.

[23] Smith J, Jones B and Brown J. The title of the journal paper. *Journal Name*, Vol. 1, No. 1, pp 1-11, 2001.

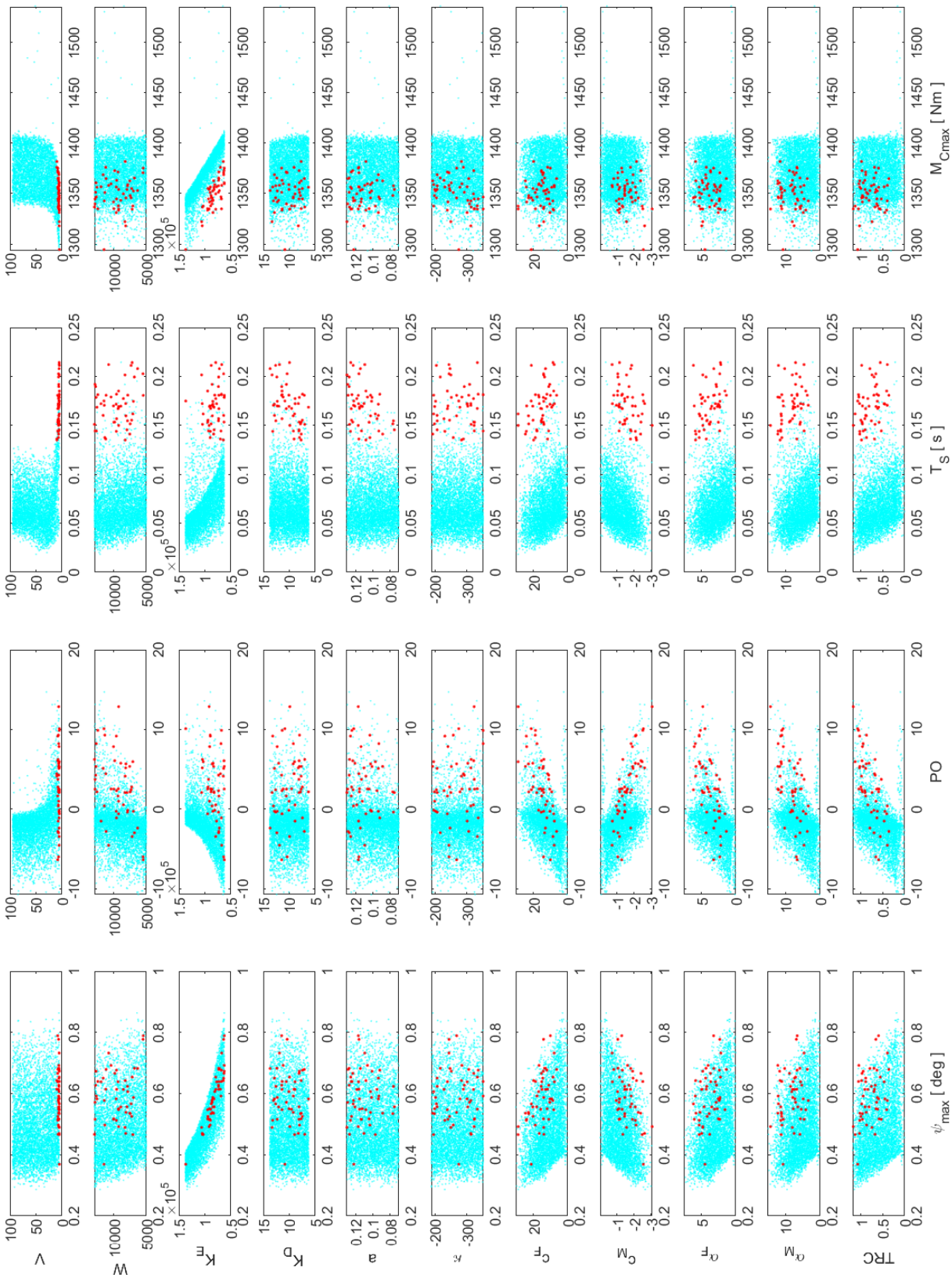

Figure 6 – Visualization of MC SRA results for PM2. Red dots are used when envelope constraint is violated.